

## ON-LINE ASPECTS OF STEREOPHOTOGRAMMETRIC PROCESSING OF SPOT IMAGES

Dr. V. Kratky  
Canada Centre for Mapping  
615 Booth Street, Ottawa, Ontario  
CANADA K1A 0E9  
Commission II

### ABSTRACT

Several aspects must be considered when processing a dynamic, time-dependent satellite imagery, such as produced by the SPOT system, in an on-line environment of photogrammetric compilation. Two major problems arise:

- the computer control of image stage positioning must cope with dynamic changes in the position and attitude of the imaging sensor and still retain its needed real-time performance;
- in the continuous compilation mode, the model heights entered on input must be defined with respect to the curvilinear coordinate system of the ellipsoidal or geoidal surface.

These and some other related issues are addressed and solutions presented, based on extensive software simulations, analysis of numerous experiments and on practical testing in an analytical plotter.

### INTRODUCTION

Background information on the SPOT satellite mission, its goals and technical parameters is available in numerous publications; here we refer to Chevrel, Weill (1981). Even before the satellite was launched in 1986 many studies analyzed the SPOT potential in the context of cartography and photogrammetry, particularly for topographic mapping. Out of existing, commercially available photogrammetric hardware, on-line photogrammetric systems are the only ones capable of handling the dynamic geometry of satellite imagery. Considerable research efforts has been carried out to demonstrate this potential by adapting analytical plotter software for accurate geometric processing of SPOT imagery, as reported by de Masson d'Autume (1980), Egels (1983), Dowman, Guban (1985), Konecny et al. (1987) and Kratky (1987,1988).

The geometry of SPOT and other satellite imageries based on the "push broom" principle differs significantly from that of photogrammetric frame cameras because their instantaneous optical imaging is restricted to a single plane containing the linear sensor. Two-dimensional image coverage is achieved by a consecutive digital collection of individual lines at a frequency roughly corresponding to the scanning resolution within the lines. Thus, the two-dimensional image is constructed as an indefinitely long strip covering the ground swath under the orbit. The constant frequency of scanning causes the image coordinate  $y'$  measured along the strip, to become actually a measure of time. Individual SPOT image scenes are arbitrary segments of the inherently continuous imagery. In contrast to frame cameras which preserve the same orientation of the three-dimensional bundle of imaging rays for the whole frame, the spatial position and orientation of the imaging sensor is continually changing along the orbit and the imaging geometry becomes dynamic and time-dependent. A rigorous geometric reconstruction of spatial relations between images and the ground scene must combine the principles of photogrammetric bundle formulation, modified in a time-dependent mode, with additional constraints derived from known orbital relations. An important objective of the solution is to properly derive and mathematically model all inherent variations in the position and attitude of the imaging sensor.

The dynamic character of imaging has its repercussions also in the process of photogrammetric compilation of SPOT images in on-line analytical instruments. The control of image positioning must effectively replicate the dynamic changes in the position and attitude of the sensor and still retain its needed real-time performance. The volume of calculations needed to update the projection centre positions and the rotation matrices involved may increase the duration of the real-time programming cycle beyond acceptable limits, unless certain time saving modifications to some of the photogrammetric algorithms are applied. Special considerations must be given to the way in which the elevations are controlled in continuous compilation of contours. The standard photogrammetric footwheel control of the measuring mark maintains a constant height in a rectangular coordinate system, while in SPOT processing it must be continuously defined with respect to the curved ellipsoidal or geoidal surface. Finally, there are some peculiarities involved in stereoviewing of SPOT uncorrected, raw images (produced at SPOT IMAGE level 1a) which are needed in a rigorous photogrammetric approach.

All these aspects are considered here in the context of formulation given by Kratky (1987) and with the use of the NRC Anaplot I on-line system.

## REAL-TIME POSITIONING

### Principles of Real-Time Positioning

On-line photogrammetric systems are photograph measuring devices interfaced with computer which can process measured information on-line with its collection. Of interest here are only closed-loop systems which not only instantly process the information, but also use it in a feedback mode to monitor and control the operation. The main element of this function is a continuous, computer-controlled real-time positioning of images. The positioning is achieved by digital means applicable to discrete points only and, in a continuous dynamic operation, it must appear physically smooth even though it is implemented by a fast repetitive cycle of digital computations. These proceed in a stream of densely spaced discrete data points defined by the operator's control of the measuring mark in the observed optical stereomodel. The computations are based on transformations between object and image spaces with the use of previously derived parameters. Included in the computations are corrections for any physical image distortions. The practically required frequency of the real-time loop is between 50 to 100 Hz. The operator retains the physical and dynamic control of the system through input control elements and, with a perfect illusion of continuity, receives his feedback from stereobservations of computer positioned image details.

### Real-Time Positioning of Photogrammetric Frame Images

Conventional photogrammetric images are taken by frame cameras specially calibrated to provide an image geometrically representing a point-by-point, straight-line projection of the object by a perspective bundle of rays passing through an ideal projection centre. The projection centre has coordinates  $X_c, Y_c, Z_c$  and the angular orientation of the bundle is defined by rotation matrix  $M$ . The basic form of an algorithm relating the individual image and photogrammetric model points is fairly simple: orthogonal transformation of rectangular coordinates of a point from one space to the other is followed by auxiliary scaling.

For image coordinates  $x', y'$ , principal distance  $f$  and model coordinates  $X, Y, Z$  the projection from model to image, MDL-IMG:  $(X, Y, Z) \mapsto (x', y')$ , is uniquely defined and implemented by a sequence of equations

$$\text{MDL-IMG: } \begin{pmatrix} U \\ V \\ W \end{pmatrix} = \mathbf{M}^T \begin{pmatrix} X - X_c \\ Y - Y_c \\ Z - Z_c \end{pmatrix}, \quad s = -f/W, \quad \begin{pmatrix} x' \\ y' \\ -f \end{pmatrix} = s \begin{pmatrix} U \\ V \\ W \end{pmatrix}, \quad (1)$$

while the opposite projection, IMG-MDL:  $(x', y', f) \mapsto (X, Y, Z)$ , is obviously not unique and must be defined for a chosen level  $Z$

$$\text{IMG-MDL: } \begin{pmatrix} x \\ y \\ z \end{pmatrix} = \mathbf{M} \begin{pmatrix} x' \\ y' \\ -f \end{pmatrix}, \quad r = (Z - Z_c)/z, \quad \begin{pmatrix} X \\ Y \\ Z \end{pmatrix} = \begin{pmatrix} X_c \\ Y_c \\ Z_c \end{pmatrix} + r \begin{pmatrix} x \\ y \\ z \end{pmatrix}. \quad (2)$$

For future comparison, it may be useful to establish the number of "hard" arithmetic operations, multiplications and divisions, involved in these basic transformations, disregarding additional calculations needed to apply system corrections, fiducial transformation, interface functions etc. Eqs. (2) include 13 of these operations (nine in matrix-vector multiplication, one division to derive scale  $r$  and three scalar-vector multiplications), while Eqs. (1) have only 12 hard operations, because scalar multiplication  $sW$  is not needed; resulting value  $-f$  is already known.

In most cases the real-time program accepts  $X, Y, Z$  model coordinates as input and applies the MDL-IMG projection into both images, the resulting  $x', y', x'', y''$  coordinates being used for the stage positioning

$$\begin{array}{l} \text{RT:} \quad x' \ y' \longleftarrow \underline{X} \ \underline{Y} \ \underline{Z} \longrightarrow x'' \ y'' \\ \text{NRT:} \quad \quad \quad \quad \quad \quad \quad \downarrow \\ \quad \quad \quad \quad \quad \quad \quad \quad \quad \quad E \ N \ h \end{array} \quad (3)$$

The upper line represents the real-time (RT) transformations while the lower line indicates an optional computation of UTM coordinates of easting  $E$  and northing  $N$ , together with ellipsoidal or geoidal elevation  $h$ , which may proceed in near real time (NRT) when the positioning process is interrupted. The input values for the RT operation are underscored. The number of needed hard operations is  $2 \times 12 = 24$ . In triangulation applications, however, a modified approach is more efficient. For instance, operator's input is  $x', y', Z$ , which means that the handwheels operate directly on the left image and the projection proceeds as IMG1-MDL-IMG2

$$\begin{array}{l} \text{RT:} \quad x' \ y' \ Z \longrightarrow \underline{X} \ \underline{Y} \longrightarrow x'' \ y'' \\ \text{NRT:} \quad \quad \quad \quad \quad \quad \quad \downarrow \\ \quad \quad \quad \quad \quad \quad \quad \quad \quad \quad E \ N \ h \end{array} \quad (4)$$

Here, the number of involved hard operations is  $13 + 12 = 25$ . Alternately, the right image may represent the primary input and the projection proceeds backwards as IMG2-MDL-IMG1. This arrangement is necessary in order to establish the known positions of tie points measured in preceding models of the bridging procedure. The practical effect of this mode of positioning is that it conveys an illusion of a stereocomparator operation in which elevation changes are interpreted as parallax displacements in one image only.

#### Real-Time Positioning of SPOT Images

The position of the projection centre and the corresponding attitude matrix  $\mathbf{M}$  are dependent on time and, therefore, can be expressed as functions of  $y'$

$$X_c = (X_c, Y_c, Z_c)^T = F_c(y') \quad , \quad a = (\alpha, \phi, \omega)^T = F_a(y') \quad , \quad M = F_M(a) \quad . \quad (5)$$

Function  $F_M$  represents the construction of a rotation matrix from three parameters and functions  $F_c$ ,  $F_a$  can be expressed as quadratic polynomials, e.g.,

$$X_c = X_0 + y' \dot{X} + y'^2 \ddot{X} \quad \text{etc.} \quad (6)$$

where  $X_0$  corresponds to the position for the centre of scene and  $\dot{X}$ ,  $\ddot{X}$  are linear, quadratic rates of change, respectively. The volume of real-time computations is obviously high, because of the need to steadily update  $F_c$ ,  $F_a$  and  $F_M$ . The projection from image to model, is then represented by an expanded sequence of equations with input variables  $x', y', Z$  as in Eqs. (2)

$$\text{IMG-MDL: } x = (x \ y \ z)^T = M(x' \ 0 \ -f)^T \quad , \quad r = (Z - Z_c)/z \quad , \quad X = X_c + rx \quad , \quad (7)$$

where  $X = (X \ Y \ Z)^T$ .

The projection from model to image, MDL-IMG:  $(X, Y, Z) \mapsto (x', y')$ , is even more complicated because functions  $F_c$ ,  $F_a$ ,  $F_M$  all depend on unknown  $y'$  which is to be derived in the same process. Consequently, the projection is not feasible in a single sequence of transformations as in Eqs. (1). An initial approximation of  $x', y'$  must be gradually refined by iterations which involve a repeated sequence of Eqs. (7) until all values  $X_c$ ,  $a$ ,  $x'$ ,  $y'$  stabilize and computed  $X$  agrees with that on input

$$\begin{aligned} \text{MDL-IMG:} \quad & \text{Estimate } x', y' \\ & \text{Repeat} \\ & \text{IMG-MDL: } (x', y')_i \mapsto (X, Y, Z)_i \\ & d(x', y')_i = ((X, Y) - (X, Y)_i) / r \\ & (x', y')_{i+1} = (x', y')_i + d(x', y')_i \\ & \text{Until } d(x', y')_i \text{ is negligible.} \end{aligned} \quad (8)$$

The number of multiplications involved in process (7) is nine for each function  $F_c$ ,  $F_a$  and about 24 in  $F_M$ , then six for the rotation and four for scaling of coordinates, the total being 52. Process (8) may need to be repeated on the average four times, which involves 216 multiplications.

To reduce the need for excessive iterations the real-time control of positioning should follow combination IMG1-MDL-IMG2 identified by schematic (4), starting with  $x', y'$  coordinates of the left image on input and project them on a desired level  $Z$  in straight forward operations (7) first. The iterative process then applies only to the projection from model to the right image. However, even in this arrangement the number of multiplications per cycle is very high; using previous estimates for Eqs. (7),(8) a total of 268 multiplications are used, which is about 11 times more than in positioning of conventional photogrammetric images.

#### Streamlining of Real-Time Programming Cycle for SPOT Images

Unless special arrangements to streamline the algorithms are found the computation time used may be too high. An obvious option may be to use an assembly language coding which would cut down on time. Yet, a higher level language programming is generally preferred for the convenience and flexibility of its use when changes are needed. Another possibility is to restrict the use of double precision mode in computations to a minimum, where absolutely necessary. In SPOT transformations the only operations and variables which warrant double precision are UTM conversions, geocentric coordinates and related scale factors and conversion constants. None of

these are needed in real-time computations and they can be run entirely in single precision preserving 6-digit accuracy. Obviously, any object time overhead is slowing down execution of a program and, consequently, calls to subroutines should be avoided by their repeated direct coding in the real-time module. A great potential for speeding up the real-time cycle is in simplifying the transformations by running a fast standard real-time program, e.g., for conventional frame images while compensating for its systematic deficiencies by applying corrections taken, or interpolated, from look-up tables prepared in advance for the full spatial range of the ground scene, as described, e.g., by Konecny (1987). Yet another alternative consists in modeling the time demanding series of rigorous transformations by polynomial expansions, thus mapping the input values into any desired output. The accuracy of this process can be controlled at a desired level by empirical testing of the transformation degree and of the form and number of included terms, as needed. This process will be demonstrated below in this paper.

It may be of interest to demonstrate some practical effects of streamlining with an example of experimental series of refinements in the positioning algorithm, as implemented by the author. Schematic (4) carried out using the formulation of Eqs. (7),(8) was programmed in Fortran 77 and the speed of the RT cycle was tested in DEC VAX 750 microcomputer by running batches of up to 1000 cycles at a time. With subroutines used for PHG-MDL conversion and for the construction of rotation matrices, and with all variables declared in double precision, a single RT cycle was measured to last 26.4 ms. After the subroutine calls for PHG-MDL were replaced by repeated direct coding, the time was reduced down to 8.1 ms. Further time reduction to 6.5 ms was achieved by reducing the size of matrix  $M$  in Eqs. (7) from (3x3) to (3x2). In the next step, all calls to subroutines were eliminated and dynamic conditions of continuous positioning were simulated by using results from a previous cycle as an approximation for the new cycle. Depending on the speed of simulated motion, the resulting cycle time was 3.8 or 2.8 ms for fast and slow positional changes in  $y''$  by 50  $\mu\text{m}$  or 5  $\mu\text{m}$  per cycle, respectively. Finally, with the whole RT program run in single precision the cycle time was brought down to 3.1 and 2.1 ms. A significant total improvement due to the streamlining of the program by a factor of ten times was clearly demonstrated. Nevertheless, in spite of the relative improvement there are still about 160 multiplications in each RT cycle. The same test program run on a PDP 11/45 minicomputer is about ten times slower, with 20 and 30 ms for the same above range of dynamic changes. Because the resulting RT frequency of 50 Hz is here just on the borderline of acceptability for an on-line operation, one more improvement was successfully tested by eliminating repeated rigorous and computationally demanding construction of orthogonal matrices from their three independent parameters. Instead, each of the 9 matrix elements is individually calculated from linear fitting functions prepared in advance. Since the matrix construction appears in the streamlined positioning cycle about three times, the saving amounted to 36 multiplications, so reducing their total number in the cycle to 124.

## ON-LINE INPUT CONTROL

### Control of Elevation Input

The task of using geoidal or ellipsoidal heights  $h$  on input to an analytical plotter involves their conversion to model coordinates  $Z$  by a series of rigorous and time consuming transformations described by Kratky (1987,1988). However, their direct implementation is practically impossible in a real-time cycle with a frequency higher than 50 Hz.

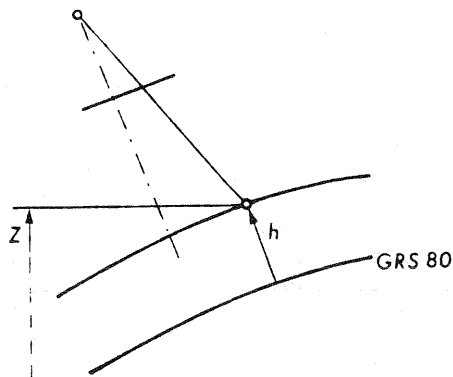


Fig.1 Projection of Imaging Rays on Reference Ellipsoid

Since the earth curvature is well pronounced in a SPOT ground scene, geoidal or ellipsoidal elevations  $h$  must be measured or followed by the Z-wheel along curved surfaces characterized by constant  $h$ , as indicated in Fig. 1. An efficient 'h-to-Z' conversion is needed on input. It can be iteratively implemented starting with an initial approximation of  $Z$ , as follows

$$\begin{aligned}
 \text{h-Z:} & \quad \text{Estimate } Z \\
 & \quad \text{Repeat} \\
 & \quad (x', y', Z)_i \longrightarrow (X, Y, Z)_i \longrightarrow (E, N, h)_i \\
 & \quad Z_i = Z_i + h - h_i \\
 & \quad \text{Until } h = h_i
 \end{aligned} \tag{9}$$

This transformation can be rigorously determined in advance for a suitable (5x5) square grid of values  $x', y'$  covering the left SPOT image, and for three levels of  $h$  extended over the full elevation range of the ground scene. Following that, a suitable polynomial function  $F_z(x', y', h)$  is derived to fit the spatial grid through a least squares solution, so defining parameters which can then be applied in real-time conversions with enormous time savings. The degree of the transformation, the number and form of needed terms were determined experimentally and yielded the following expression

$$Z = F_z(x', y', h) = (1 \ h \ x \ y \ hx \ xy \ x^2 \ y^2 \ x^3) \mathbf{a} = \mathbf{p}_z^T \mathbf{a} \quad , \tag{10}$$

where  $\mathbf{a}$  is a vector consisting of parameters  $a_1$  to  $a_9$ , and  $\mathbf{p}_z$  - vector of nine corresponding polynomial coefficients formed from chosen  $(x, y, h)$  power combinations. The number of multiplications in Eq. (10) can be reduced from 14 to 8 by a proper grouping of terms, for instance

$$Z = a_1 + h(a_2 + a_5x) + x(a_3 + x(a_7 + a_9x)) + y(a_4 + a_6x + a_8y) \quad . \tag{10a}$$

The formulation easily meets the real-time requirements and provides an excellent accuracy. Absolute errors of the transformation are within  $|dZ| < 0.2$  m for the range of  $\Delta h = 1$  km and within  $|dZ| < 0.7$  m for  $\Delta h = 4$  km, both cases being computed for the maximum side viewing angle  $27^\circ$  of the imaging sensor.

Using this approach, schematic (4) for real-time positioning of SPOT images should now be changed to a new form in which the number of needed multiplications increases from 124 to 132

$$\begin{array}{l}
 \text{RT:} \quad \underline{x'} \ \underline{y'} \ \underline{h} \ \longmapsto \ X \ Y \ Z \ \longmapsto \ x'' \ y'' \\
 \text{NRT:} \quad \quad \quad \quad \quad \quad \quad \downarrow \\
 \quad \quad \quad \quad \quad \quad \quad \quad \quad \quad E \ N
 \end{array} \tag{11}$$

#### GENERALIZED CONTROL BY FITTING FUNCTIONS

The same principle of polynomial modeling can be applied to computations of other variables in the real-time process. The most useful application in this regard is its substitution for the rigorous composite transition from the left to right image, IMG1-MDL-IMG2. Experiments demonstrated an excellent performance of a single step of mathematical mapping with an 11-term polynomial for  $x''$  and 9-term polynomial for  $y''$

$$x'' = F_x(x', y', h) = (1 \ h \ x \ y \ hx \ hy \ xy \ x^2 \ y^2 \ x^2y \ x^3) \mathbf{d} = \mathbf{p}_x^T \mathbf{d} \quad , \tag{12}$$

$$y'' = F_y(x', y', h) = \mathbf{p}_y^T \mathbf{e} \quad , \tag{13}$$

where  $\mathbf{d}$  and  $\mathbf{e}$  are corresponding vectors of parameters. Functions (12), (13) were tested for stereopairs of SPOT images corresponding to ratio  $b/h = 0.5$ , that is for the combination of viewing angles  $0^\circ$  and  $27^\circ$ . The accuracy of  $F_y$  is excellent for any practical range  $\Delta h$ , leaving maximum absolute errors within  $|dy''| < 0.2 \ \mu\text{m}$ . Maximum absolute errors of  $x''$  are as follows:  $|dx''| < 0.5 \ \mu\text{m}$  for the range of  $\Delta h = 2 \ \text{km}$ ,  $dx'' < 1.0 \ \mu\text{m}$  for  $\Delta h = 4 \ \text{km}$  and they increase into micrometres for higher ranges of elevations. For these, practically rare ground conditions polynomial function  $F_x$  should be expanded by inclusion of a term with coefficient  $h^2$ . Similarly to the arrangement in Eq. (10a) the number of multiplications for the 11-term polynomial expression in Eq. (12) can be reduced from 19 to 10. For the combination of two oblique SPOT images and corresponding  $b/h = 1$ , the inaccuracies in  $x'', y''$  will increase two times and the use of term with  $h^2$  becomes more critical.

Quite logically, when already computing the raster of rigorous Z-values in Eqs. (9) needed for polynomial formulation (10), one can also store values X, Y and derive their equivalent fitting functions with 11-terms

$$X = F_x(x', y', h) = (1 \ h \ x \ y \ hx \ hy \ xy \ x^2 \ y^2 \ hx^2 \ x^3) \mathbf{b} = \mathbf{p}_x^T \mathbf{b} \quad , \tag{14}$$

$$Y = F_y(x', y', h) = \mathbf{p}_y^T \mathbf{c} \quad , \tag{15}$$

where  $\mathbf{b}$ ,  $\mathbf{c}$  are 11-component vectors of parameters for the computation of X, Y, respectively. Parameter grouping equivalent to that of Eq. (10a) will allow conversions of X, Y to be implemented with only 10 multiplications each. The accuracy of these transformations is also excellent; maximum absolute errors in X and Y are smaller than 0.3 m for any practical range of elevations.

Eventually, the near real-time computation of UTM coordinates E, N should be arranged by similar fitting functions of  $(x', y', h)$  to save computing time and to circumvent the computation of intermediate model values X, Y, Z. The concept of real-time positioning of images in analytical plotters can then be fully based on direct polynomial mapping of all needed conversions and the original schematics of consecutive projections (4) or (11) are replaced by a set of independent mapping functions

$$\begin{array}{l}
 \text{RT:} \quad \underline{x'} \ \underline{y'} \ \underline{h} \ \longmapsto \ x'' \ y'' \\
 \quad \quad \quad [ \ \underline{x'} \ \underline{y'} \ \underline{h} \ \longmapsto \ X \ Y \ Z \ ] \\
 \text{NRT:} \quad \underline{x'} \ \underline{y'} \ \underline{h} \ \longmapsto \ E \ N \\
 \quad \quad \quad [ \ X \ Y \ Z \ \longmapsto \ E \ N \ ]
 \end{array} \tag{16}$$

relating the input image space to any other needed coordinate space through

chosen elevation  $h$ . The two lines enclosed in brackets represent options. In this arrangement, the real-time positioning loop can be implemented with no compromise in rigor or accuracy with only 18 multiplications and is almost seven times faster than that of the streamlined approach. Its performance ultimately surpasses even that of the standard loop for frame images. Table 1 presents an overview of the number of multiplications in individual cases discussed above.

Table 1

Number of Multiplications Involved in Different RT Formulations

Process	Equations	Number
Standard RT Positioning - FRAME	(1)	24
Straight RT Positioning - SPOT	(7),(8)	268
Streamlined RT Positioning - SPOT	(7),(8)	124
Streamlined RT Positioning - SPOT	(7),(8),(10)	132
Generalized RT Positioning - SPOT	(12),(13)	18

#### CHARACTER OF SPOT GEOMETRY

To demonstrate practically the relation of and the differences in two SPOT stereoisimages of the same ground scene, an example of fictitious data was generated. The left image was chosen as vertical, the right image was oblique, pointed  $25^\circ$  due west, and the geographic latitude of the scene  $\phi = 46^\circ$ . In the left image considered in the physical size ( $s = 78$  mm) of the sensor's linear array, a (5x5) square reference grid was adopted, which was projected first to a zero level of the GRS 80 reference ellipsoid and then back into the tilted right image, respecting the orbital motions of the satellite and an ideal attitude control of the sensor. Rigorous spatial transformations were applied throughout the calculations. The distorted grid pattern is non-linear and corresponds to the effect of Eqs. (12),(13). Fig. 2 is a graphical representation of the square reference pattern for the left image and of the distorted corresponding grid of the right image, when coordinate axes of both images are superimposed. The maximum absolute differences in coordinates of corresponding points are 10.6 mm for  $x'$  and 2.3 mm for  $y'$ . Local  $x$ - and  $y$ -segments of the reference grid are distorted in the right image both in scale and rotation. The most noticeable is the change of  $x$ -scale causing image compression of 20%, while the  $y$ -scale is practically unchanged. Both  $x$ - and  $y$ -segments are rotated clockwise, however, the  $x$ -rotation is more pronounced and this results in a shearing effect, changing the original right angles of the grid. All these changes vary continuously. Table 2 summarizes the range of the variations and their average values.

Table 2

Change in Geometry by Projecting Vertical into Oblique SPOT Image

Change	Scale of Segments		Rotation of Segments		Skew angle y-to x
	in x	in y	in x	in y	
Minimum	0.767	1.000	$-4.01^\circ$	$-2.68^\circ$	$1.12^\circ$
Average	0.795	1.000	$-4.16^\circ$	$-2.79^\circ$	$1.37^\circ$
Maximum	0.823	1.000	$-4.32^\circ$	$-2.91^\circ$	$1.61^\circ$

The spread of variable distortion is reasonably small and does not cause any special concerns with regard to the optical conditions of stereobobservation



of SPOT raw image transparencies. The viewing field rotation can be optically adjusted for the whole SPOT image and the remaining variations and skewness are not significant enough to affect the observation comfort. There is no need to apply computer control of visual field rotation available in some analytical plotters. Equal scale of y-segments warrants that no residual y-parallaxes will appear in the periphery of the optical field of view, when their centres are either manually adjusted or are under computer control.

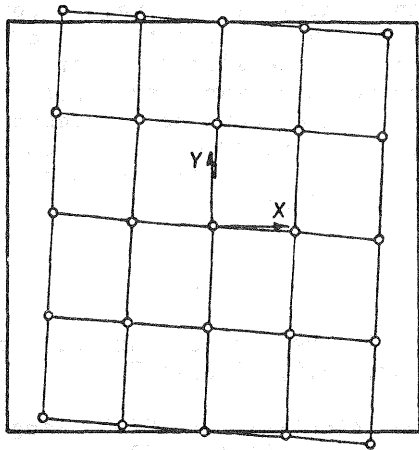


Fig. 2 Distortion of SPOT Image

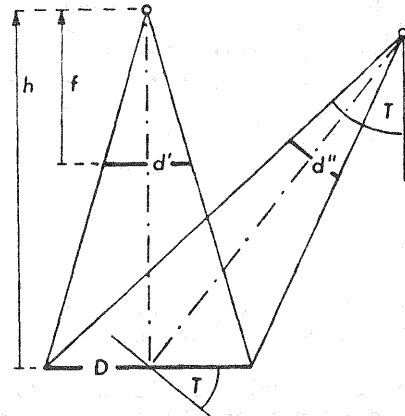


Fig. 3 Compression of Oblique Image

The only serious practical problem arises from the x-scale compression of the tilted SPOT image, which considerably affects the stereobservations. As a result of the change in scale of two images which are supposed to be merged in the process of stereoperception, one perceives x-parallaxes increasing towards the periphery of the viewing field and the stereomodel becomes considerably slanted in the x-direction. As seen from Table 2, the variations of this scale change over the whole image area are only +0.028 and if the average x-scale were corrected when reproducing the transparencies, the problem would be resolved. Fig. 3 illustrates the conditions under which SPOT images are taken. Ground segment D is projected into d' or d'' in a vertical or oblique image, respectively

$$d' = D.f/h \quad , \quad d'' = D \cos^2 T . f/h \quad ,$$

where f is the focal length of the imaging system and h - flying altitude. Scale distortion m causing x''-compression can be estimated by comparing both image segments

$$m = 1 + dm = d''/d' = \cos^2 T = 1 - \sin^2 T \quad . \quad (17)$$

Scale error dm is always negative and is a function of tilt T of the sensor. Consequently, needed reproduction scale r or scale correction dr to be applied during the reproduction process, can be derived as

$$r = 1/m = 1/\cos^2 T \quad \text{or} \quad dr = \tan^2 T \quad . \quad (18)$$

Obviously, the distortion is identical for positive or negative tilts of the same size and is not critical for the geometrically optimal, double convergent SPOT image pairs with base-to-height ratio of 1. It is the difference between the absolute values of tilts T which causes problems. Even then, scale errors of up to 5%, corresponding to  $T = 13^\circ$ , can still be disregarded. For extreme vertical-oblique combinations, one has to use transparencies whose x-scale is compensated as shown by Eq. (18).

## CONCLUSIONS

The dynamic character of SPOT images complicates the implementation of the algorithms for rigorous real-time positioning of image stages in on-line photogrammetric operations. The number of multiplications in a single real-time cycle is 268, about 11 times higher than in standard positioning of aerial frame images. With special arrangements adopted in program coding and with some algorithmic modifications, the volume of multiplications can be reduced to 124 per cycle. A significant improvement is achieved through modeling of rigorous iterative transformations by a direct polynomial mapping of input-to-output values. A concept of a generalized control of real-time operations for analytical on-line instruments was developed and tested. With its use the real-time positioning cycle can be implemented with 18 multiplications only. The process is extended to control photogrammetric motions defined with respect to curved geodetic surfaces, as needed for measurements of ellipsoidal or geoidal heights.

## REFERENCES

- Chevrel, M. and G. Weill, 1981. The SPOT Satellite Remote Sensing Mission. *Photogrammetric Engineering and Remote Sensing*, 47(8): 1163-1171.
- Dowman, I.J. and D.J. Gagan, 1985. Application Potential of SPOT Imagery for Topographical Mapping. *Advanced Space Research*, 5(5):73-79.
- Egels, Y., 1983. Amélioration des logiciels TRASTER: restitution d'images à géométrie non conique. *Bull. Inf. IGN*, 1983(2):19-22.
- Konecny, G., P. Lohmann, H. Engel and E. Kruck, 1987. Evaluation of SPOT Imagery on Analytical Photogrammetric Instruments. *Photogrammetric Engineering and Remote Sensing*, 53(9):1223-1230.
- Kratky, V., 1987. Rigorous Stereophotogrammetric Treatment of SPOT Images. *Actes du Colloque International "SPOT1 - Utilisation des images, bilan, Résultats"*, CNES, Paris.
- Kratky, V., 1988. Universal Photogrammetric Approach to Geometric Processing of SPOT Images. *International Archives of Photogrammetry and Remote Sensing*, 27(4), ISPRS, Kyoto.
- de Masson d'Autume, M.G., 1980. Le traitement géométrique des images de télédétection. *Annales des Mines* 1980(2):53-62.